

Original Article

---

# Capability of constructive interference in steady state sequence versus postcontrast T1-weighted imaging in cerebellopontine angle and internal auditory canal masses

*Vorawan Charoonratana, M.D.*

*Nuttha Sanghan, M.D.*

*Siriporn Hirunpat, M.D.*

*Kornpen Rattanaprueksachart, M.D.*

From Department of Radiology, Faculty of Medicine, Prince of Songkla University, Hat Yai, Songkhla, Thailand.

Address correspondence to V.C. (e-mail: vorawan62@outlook.com)

Received 5 January 2023; revised 8 April 2023; accepted 15 April 2023  
doi:10.46475/aseanjr.v24i1.205

## Abstract

**Background:** The tumor size is one of the main factors in the treatment of cerebellopontine angle (CPA) tumors, and magnetic resonance imaging (MRI) with gadolinium-based contrast agent (GBCA) provides the best evaluation. However, administration of the gadolinium is time consuming and increasing in cost. There is a risk of nephrogenic systemic fibrosis in patients with renal failure and liver or renal transplantation.

**Objective:** The purpose of this study was to assess the capability of constructive interference in steady state (CISS) sequence in measuring the tumor size of the CPA and internal auditory canal (IAC) masses compared to postcontrast T1-weighted images (T1-WI).

**Materials and Methods:** The 118 MR studies with both CISS sequence and postcontrast T1-WI of 45 patients with CPA and IAC masses were retrospectively reviewed.

**Results:** There was no significant difference between CISS and postcontrast T1-WI in measuring size in transverse diameter of the masses ( $p = 0.051-0.06$ ). The longitudinal diameter measurement revealed a significant difference ( $p < 0.001$ ) and the measured size on postcontrast T1-WI was slightly larger than the CISS image. The difference in median measurement between two sequences was less than 0.9 mm. and Bland-Altman plots revealed that differences between the two sequences in longitudinal and transverse diameters of the masses were within the limits of agreement. Interobserver agreement showed excellent correlation ( $r = 0.994-0.999$ ,  $p < 0.001$  by Pearson's product-moment correlation).

**Conclusion:** The CISS sequence may be sufficient for assessing the size of CPA and IAC masses, which can be used interchangeably with postcontrast T1-weighted image as a contrast-free option, especially in follow-up studies and vulnerable settings of gadolinium administration.

**Keywords:** CISS sequence, CPA tumor, IAC mass, Magnetic resonance imaging, Tumor size.

## Introduction

Cerebellopontine angle (CPA) tumors account for 5%-10% of intracranial tumors in adults and 1% of all pediatric intracranial tumors [1]. The vast majority of CPA and internal auditory canal (IAC) masses are vestibular schwannomas (VSs), 80%-90% [2-3]. For VSs, magnetic resonance imaging (MRI) provides high sensitivity and specificity, up to 100% and 92.8% respectively [4]. Regarding natural history, 66% of VSs show no progression and 23% spontaneously regress [4-5]. Meningiomas are the most common intracranial extra-axial tumors in adults and the second most frequent lesions in the CPA cistern after VSs, 10%–15% [6]. They can extend into the IAC and are mostly slow growing. For CPA-IAC tumors,

treatments and surgical approaches are based on multiple factors. The tumor size is one of the main factors and MRI provides the best evaluation [7-9]. MRI with gadolinium-based contrast agent (GBCA) is a non-invasive tool to identify the site and extension of the lesions, characteristic signal intensity, monitor disease progression, and pre-operative and post-operative assessments [4, 10]. A follow-up interval is variable and dependent on clinical consideration because 58.6% of patients had an annual tumor growth rate of less than 1 mm/year [11]. According to a meta-analysis study [12], the average length of imaging follow-up was 3.2 years.

However, administration of the GBCA is time consuming and increasing in cost. In addition, there are associations of GBCA and nephrogenic systemic fibrosis (NSF) in patients who had renal failure and liver or renal transplantation [13]. Furthermore, intravenous GBCA exposure and multiple GBCA administrations are associated with neuronal tissue deposition [14-15]. Avoiding GBCA exposure by using non-gadolinium based study is preferable in patients who tend to have long-term imaging follow-up for slow growing lesions. The constructive interference in steady state (CISS) sequence is a balanced steady-state free precession (bSSFP), which is a heavily fluid-weighted 3D sequence used with isotropic or near isotropic spatial encoding. The bSSFP technique has been shown to be useful in screening and evaluation for vestibular schwannomas, with a sensitivity of 94% and a specificity of 97% [16-18]. This study assumed that it could be applied to the other CPA and IAC tumors as well as schwannomas [19]. For this reason, this study aimed to determine whether it is possible to use the CISS sequence as a gadolinium-free alternative tool in measuring the tumor size of the CPA-IAC masses.

## Materials and methods

### Study design and target population

This retrospective review of patients who had CPA-IAC masses and MRI studies with IAC protocol from January 2011 to December 2015, was approved by an institutional review board. The inclusion criteria required the MRI, which provided CISS and postcontrast T1-weighted images (T1-WI), on the same date. Patients less than 15 years of age were excluded according to different incidences of diseases. A patient who had an epidermoid cyst was also excluded because it did not typically enhance.

The total of 45 patients were enrolled in our study, 26 females and 19 males with the mean age of 54 years (range: 24-78 years). Among them, 22 patients (48%) underwent operations. The patients had follow-up studies ranging from 1-7 times. The follow-up interval was from three months up to two years. The total of 118 MRI studies, including initial and follow-up images, met the criteria. There were 58 post-operative studies and 60 non-operative images.

Most patients had a solitary IAC-CPA mass. Two patients were diagnosed with neurofibromatosis type 2, one had bilateral vestibular schwannomas and the other had a left vestibular schwannoma with bilateral trigeminal schwannomas. Thus, overall, 46 masses were detected in CPA-IAC regions; 42 were vestibular schwannomas, and 4 were meningiomas by a provisional diagnosis with 22 pathological diagnoses. Regarding tumor locations, 25 masses had only intracanalicular portions. Four masses were located only in the CPA cisterns without IAC involvement, and the rest occupied both intracanalicular and cisternal portions.

### Image acquisition

The MRI studies were performed with either a 3.0-Tesla (T) (AchievaR, Philips) or a 1.5T scanner (IngeniaR, Philips) with a standard head coil. The protocol included the whole brain axial fluid attenuation inversion recovery (FLAIR), diffusion weighted imaging (DWI) and postcontrast T1-WI in 3 views, and

thin slice of temporal bone consisting of T1-WI, T2-weighted image (T2-WI), DWI and CISS in the axial plane, T1-WI and T2-WI in the coronal plane and postcontrast T1-WI with fat suppression in axial and coronal views. The axial CISS 3D images were performed with the following parameters: repetition time (TR)/echo time (TE) 1500 ms/180 ms, with 1 mm section thickness, NEX 2, Matrix 127x256. The axial spin-echo T1W of the temporal bone was obtained following the parameters: TR/TE 500 ms/10 ms, with 2 mm section thickness, NEX 4, Matrix 180x252. The post-contrast images were obtained after injection of 0.1 mmol/kg of GBCA (Gadobutrol).

### **Reader assessment method**

Two neuroradiologists (with 5 and 2 years of experience), independently interpreted MRI studies (initial scans and follow-up studies) of the 45 patients. The tumors were identified and a provisional diagnosis was made by a standard protocol in the case of initial scans. The tumor was divided into two parts, intracanalicular and CPA cisternal portions by using porus acusticus as a cut point. Each portion was assessed and measured separately as follows:

The intracanalicular portion was measured in parallel and perpendicular plane to the IAC as longitudinal and transverse diameters, respectively (Figure 1).

The CPA cisternal portion was measured in the parallel and perpendicular plane to the petrous part of the temporal bone and defined as longitudinal and transverse diameters, respectively (Figure 2). The measurement was made according to the suggestion of Walsh et al. [20], who revealed that the tumor grows along the axis of the canal.

The diameters of the CPA-IAC tumors were obtained only in the axial plane on the CISS and postcontrast T1-WI because the standard protocol in our institute does not provide CISS in coronal and sagittal planes.

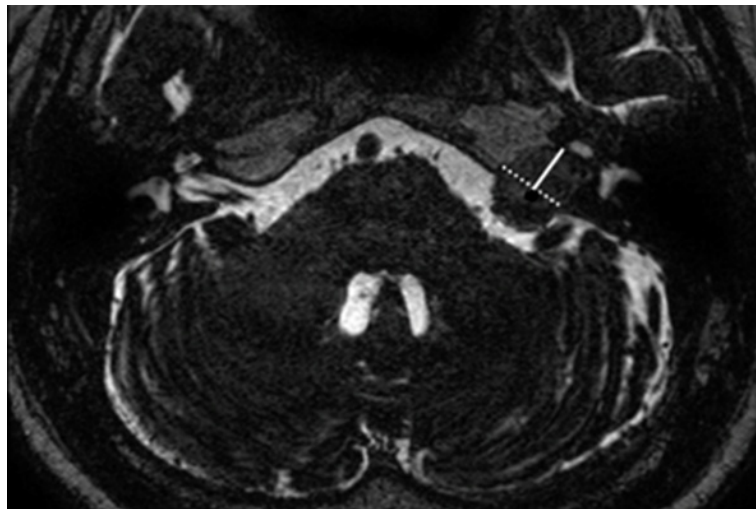


**Figure 1.** Axial 3D-constructive interference in a steady state (CISS) image shows a tumor occupying in the left internal auditory canal (IAC) and cerebellopontine angle (CPA) cistern. The longitudinal diameter (solid line) and transverse diameter (dotted line) of IAC portion are parallel and perpendicular to the IAC. Porus acusticus (opening of the IAC) is a borderline between the CPA and IAC portions.

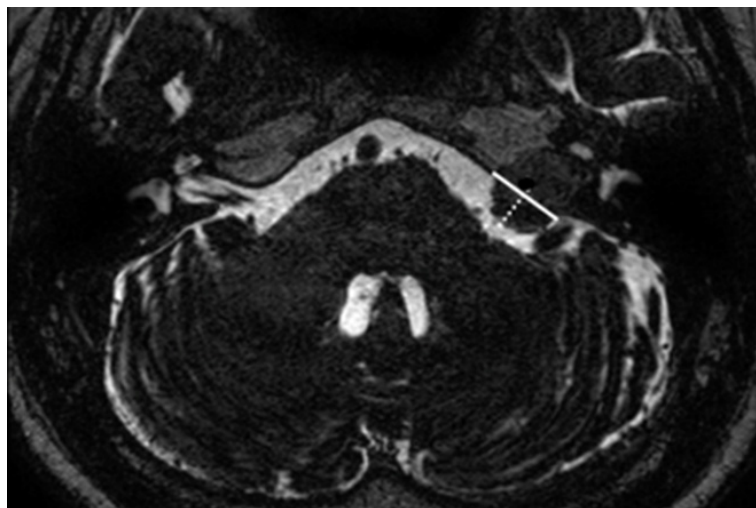


**Figure 2.** Axial 3D-constructive interference in a steady state (CISS) image shows a tumor occupying in the left internal auditory canal (IAC) and cerebellopontine angle (CPA) cistern. The longitudinal diameter (solid line) and transverse diameter (dotted line) of CPA cisternal portion are parallel and perpendicular to the petrous part of the temporal bone.

### Statistical analysis

The data distribution was analyzed with the Shapiro-Wilks Normality Test. A statistical evaluation of the measurement was performed with paired Wilcoxon signed rank test in data that did not fit normal distribution and a paired t-test was used in normally distributed data. A p-value < 0.05 indicated a statistically significant difference. Bland-Altman plots were constructed to assess the measures of agreement between the two sequences by studying the mean difference and constructing limits of agreement. Interobserver correlation was evaluated using Pearson product-moment correlation coefficient (Pearson's correlation).

### Results

No significant differences between the CISS and postcontrast T1-WI in measuring the tumor size except the longitudinal diameter in both CPA and IAC portions, (p < 0.001), and transverse diameter obtained by reader 2 (p = 0.04), are detailed in Table 1. The difference in median diameter on CISS and postcontrast T1-WI in both diameters of CPA cisternal and IAC portions ranged from 0.1-0.9 mm. The measured size on postcontrast T1-WI were slightly larger than on CISS images in all diameters except the longitudinal diameter of the IAC portion, obtained from reader 1, which is summarized in Table 1.

**Table 1.** Comparison of measurement in longitudinal and transverse diameters in IAC and CPA portions of each reader.

		CPA				IAC			
		Reader 1		Reader 2		Reader 1		Reader 2	
		Median (Q1,Q3)	p-value	Median (Q1,Q3)	p-value	Median (Q1,Q3)	p-value	Median (Q1,Q3)	p-value
Longitudinal diameter	CISS	12.92 (11.04,17.32)	<0.001	12.90 (11.05,17.36)	<0.001	9.43 (6.01,11.40)	<0.001	9.43 (6.00,11.48)	<0.001
	contrast	13.72 (11.60,17.88)		13.76 (11.55,17.80)		9.30 (6.13,11.74)		9.53 (6.14,11.72)	
Transverse diameter	CISS	9.87 (7.12,14.23)	0.06	9.85 (7.13,14.12)	0.052	9.38 (7.48,13.39)	0.051	9.25 (7.50,13.40)	0.04
	contrast	10.59 (7.30,14.20)		10.55 (7.30,14.05)		9.68 (7.52,13.26)		9.70 (7.51,13.26)	

A subgroup analysis was summarized in Table 2. Regarding tumor locations, six patients (5.08%) found the tumors confined only to the CPA cisterns, tumor size measurement in longitudinal and transverse diameters showed no significant difference between CISS and postcontrast T1-WI ( $p = 0.06-0.16$ ). While only the IAC was occupied by the tumors in 67 patients (56.78%), there was a significant difference in longitudinal and transverse diameters ( $p < 0.05$ ). From 58 post-operative studies, the results showed that measurements in all diameters were not significantly different ( $P = 0.11-0.03$ ). While conservative or non-operative tumors were not significantly different in the transverse diameter of IAC measurement ( $p = 0.18$ ).

**Table 2.** *P value of subgroup categorizations, comparing each diameter measurement in CPA and IAC portion on CISS and postcontrast T1-weighted images obtained by both readers.*

	Total (n=118)	CPA				IAC			
		Reader 1		Reader 2		Reader 1		Reader 2	
		Longitudinal	transverse	Longitudinal	transverse	longitudinal	transverse	longitudinal	transverse
Tumor confined in CPA	6	0.06	0.16	0.06	0.15	N/A	N/A	N/A	N/A
Tumor confined in IAC	67	N/A	N/A	N/A	N/A	<0.001	0.03	0.001	0.03
Post-operative tumor	58	0.29	0.31	0.23	0.33	0.11	0.11	0.14	0.10
Conservative tumor	60	<0.001	0.02	<0.001	0.01	0.001	0.18	0.001	0.18

Bland-Altman plots (Figures 3 and 4) were also used to assess agreement between measurements in both sequences for longitudinal and transverse diameters of each CPA and intracanalicular portions. The plots revealed that differences between the two sequences in longitudinal and transverse diameters of CPA and IAC were within the limits of agreement; therefore, both sequences could be used interchangeably.

Interobserver agreement ranged between 0.994-0.999 ( $p < 0.001$ ), by Pearson's product-moment correlation, for measurement in all diameters of both CPA and intracanalicular portions on CISS and postcontrast T1-WI. The results implied an excellent correlation between two readers.

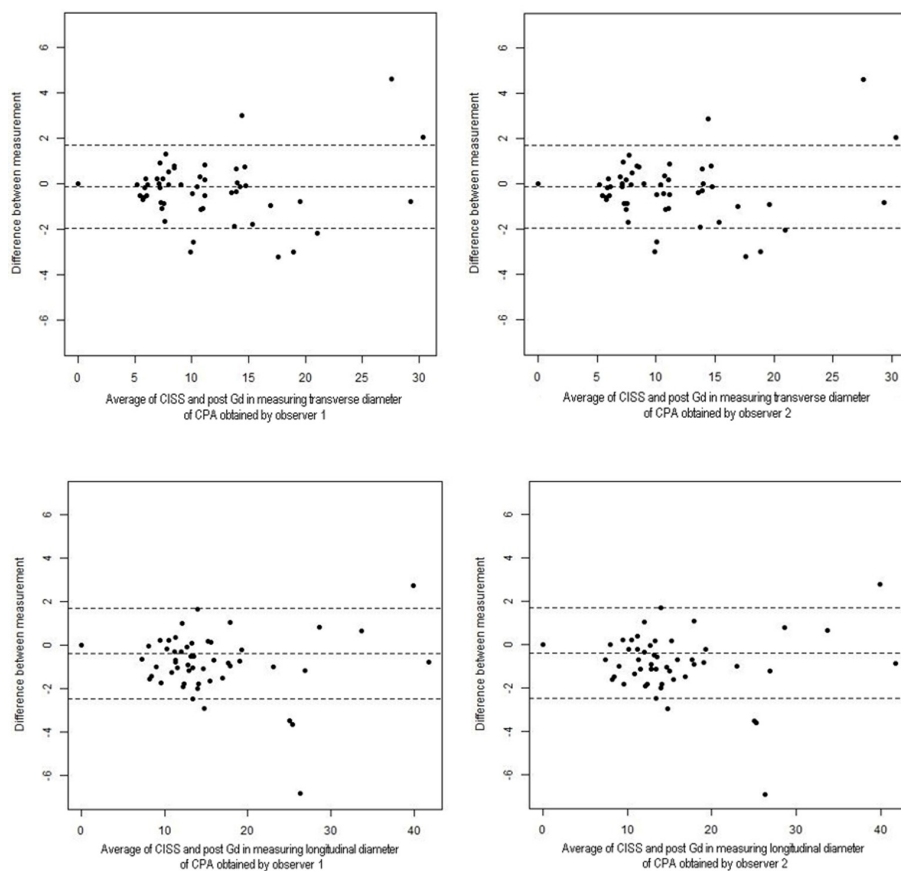


**Figure 3.** Bland-Altman plots revealed the difference and average values of tumor measurement in CISS and postcontrast T1-weighted images in the cerebellopontine (CPA) portion.

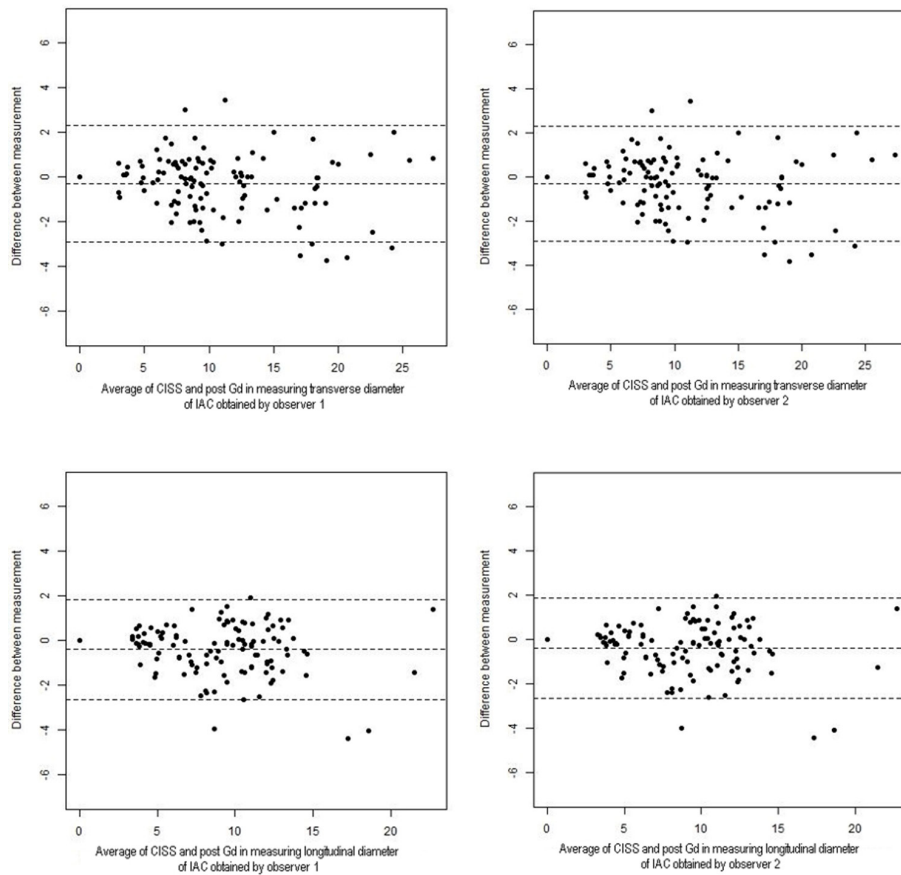


**Figure 4.** Bland-Altman plots revealed the difference and average values of tumor measurement in CISS and postcontrast T1-weighted images in the internal auditory canal (IAC) portion.

## Discussion

The goal of this study was to assess the capability of CISS sequence in measuring the tumor size of CPA-IAC masses as an effective tool compared to postcontrast T1-WI. The overall difference of both sequences in each median diameter was acceptable, less than 0.9 mm, and Bland-Altman plots also showed data was within the limits of agreement. However, a statistically significant difference in longitudinal diameter of CPA cisternal and IAC portions of both readers in addition to transverse diameter of IAC portion of reader 2 could be affected by several factors.

According to tumor locations, our study included many large IAC tumors. Most of them totally occupied the IACs and partially extended into the temporal bones. Thus, the tumor margins were hardly outlined and distinguished from the adjacent structures in CISS image (Figure 5). Additionally, signal changes in the perilymphatic fluids of the inner ear as a result of elevated protein concentration attributed to blood-inner ear barrier disruption in VSs could reveal decreased signal intensity in the ipsilateral cochlea and vestibule on CISS image [21]. For this reason, gadolinium-enhanced image was necessary to evaluate inner ear extension in particular extensive tumors whereas most small IAC lesions were clearly depicted in CISS sequence due to high signal of the cerebrospinal fluid (CSF) outlining as natural contrast. Similarly, the measurement of CPA tumor showed no difference in both sequences because the CPA tumors were clearly depicted due to high signal contrast between the tumor margin and CSF in the CPA cistern. Even though a large tumor compressed upon the cerebellar hemisphere, there was a thin CSF cleft to delineate the tumor margin.

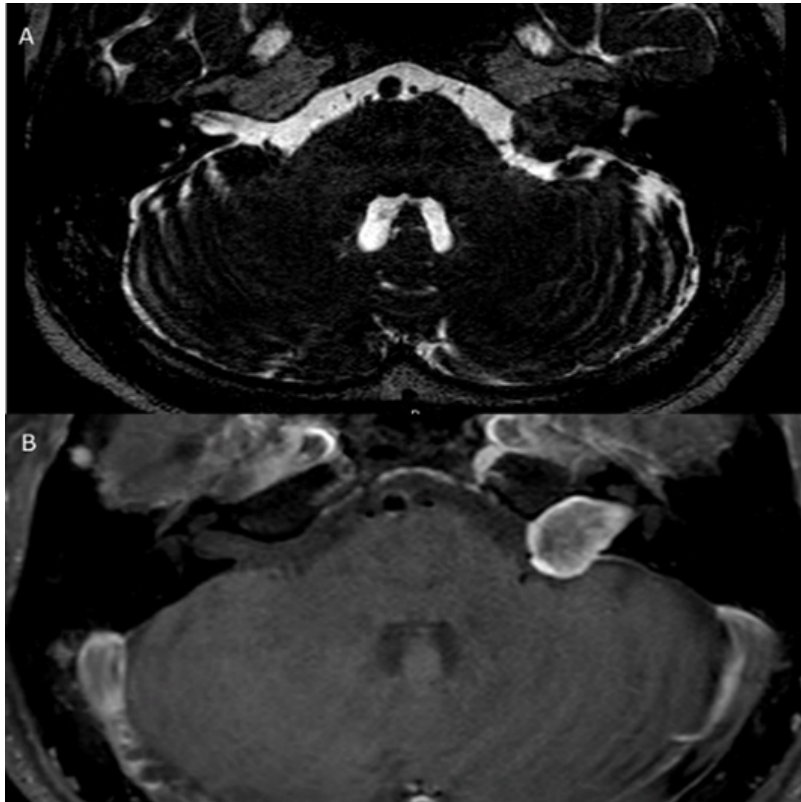


**Figure 5.** (A) Axial CISS image shows the tumor totally occupied and expanded to the left internal auditory canal (IAC). Its margin is inaccurately separable from the left temporal bone and inner ear structures without CSF signal outlining. (B) Axial postcontrast T1-weighted image clearly depicts the well-defined tumor.

The post-operative groups showed no significant difference in both CISS and contrast-enhanced sequences in all diameter measurements. However, some post-operative residual tumors showed a heterogeneous signal (cystic changes, necrotic portion) combined with the distortion of the surrounding structures. CISS occasionally could not clearly depict the outline of tumors. Conversely, some tumors showed false positive findings on contrast-enhanced images due to enhancement of the surrounding structures from post-operative changes, post-inflammation, or clustering of the internal auditory canal nerve and vascular complex [16, 22, 23]. Therefore, post-operative evaluation with CISS sequence alone should be carefully performed in some patients.

Considering tumor types, vestibular schwannomas were the main population influencing the overall data. The prior studies [16-18, 22] reported high accuracy of CISS in detection and follow-up tumor size of VSs but the large tumors or neurofibromatosis type 2 was not included. In this study, the measurement of some large tumors and multiple schwannomas in patients who had neurofibromatosis type 2 was variable and differed between CISS and postcontrast T1-WI. The range of mean difference varied from 1-7 mm in those large tumors. Thus, in these particular cases of large intracanalicular portions or extensive involvement into the temporal bone, a follow-up of the contrast studies was suggested. Regarding meningioma, it revealed no significant difference in measurement of CPA and transverse diameter in IAC portion. Most meningiomas provided a sharp boundary to the tumors, so CISS can be used as an alternative sequence to measure tumor size. However, this study had a limited number of meningiomas. In any future study, larger numbers would be required.

The limitation of this study was invariable tumor types and the difference of slice thickness between axial CISS and postcontrast T1-WI. Regarding a retrospective review, CISS sequence was performed routinely in cases of temporal bone and cranial nerve studies in our institute. Thus, other possibilities such as cases of meningiomas or metastases did not have this sequence and thus, were not enrolled in the study.

## Conclusion

In conclusion, the constructive interference in a steady state sequence may be sufficient for assessing the size of cerebellopontine angle and internal auditory canal masses, which can be used interchangeably with postcontrast T1-weighted images as a contrast-free option, especially in follow-up studies and vulnerable settings of gadolinium administration.

## References

1. Yilmaz C, Altinors N, Sonmez E, Gulsen S, Caner H. Rare lesions of the cerebellopontine angle. *Turk Neurosurg* 2010;20:390–7. doi: 10.5137/1019-5149.JTN.2961-10.0.
2. Kankane VK, Warade AC, Misra BK. Nonvestibular schwannoma tumors in the cerebellopontine angle: A single-surgeon experience. *Asian J Neurosurg* 2019;14:154-61. doi: 10.4103/ajns.AJNS\_335\_17.
3. Springborg JB, Poulsgaard L, Thomsen J. Nonvestibular schwannoma tumors in the cerebellopontine angle: a structured approach and management guidelines. *Skull Base* 2008;18:217–28. doi: 10.1055/s-2007-1016959.
4. Singh K, Singh MP, Thukral C, Rao K, Singh K, Singh A. Role of magnetic resonance imaging in evaluation of cerebellopontine angle schwannomas. *Indian J Otolaryngol Head Neck Surg* 2015;67:21–7. doi: 10.1007/s12070-014-0736-0.
5. Cavada MN, Lee MF, Jufas NE, Harvey RJ, Patel NP. Intracanalicular vestibular schwannoma: a systematic review and meta-analysis of therapeutics outcomes. *Otol Neurotol* 2021;42:351-62. doi: 10.1097/MAO.0000000000002979.
6. Bonneville F, Savatovsky J, Chiras J. Imaging of cerebellopontine angle lesions: an update. Part 1: enhancing extra-axial lesions. *Eur Radiol* 2007;17:2472–82. doi: 10.1007/s00330-007-0679-x.
7. Lin EP, Crane BT. The management and imaging of vestibular schwannomas. *AJNR Am J Neuroradiol* 2017;38:2034-43. doi: 10.3174/ajnr.A5213.
8. Silk PS, Lane JI, Driscoll CL. Surgical approaches to vestibular schwannomas: what the radiologist needs to know. *Radiographics* 2009;29:1955–70. doi: 10.1148/rg.297095713.

9. Hentschel M, Rovers M, Markodimitraki L, Steens S, Kunst H. An international comparison of diagnostic and management strategies for vestibular schwannoma. *Eur Arch Otorhinolaryngol* 2019;276:71-8. doi: 10.1007/s00405-018-5199-6.
10. Hentschel MA, Kunst HPM, Rovers MM, Steens SCA. Diagnostic accuracy of high-resolution T2-weighted MRI vs contrast-enhanced T1-weighted MRI to screen for cerebellopontine angle lesions in symptomatic patients. *Clin Otolaryngol* 2018;43:805-11. doi: 10.1111/coa.13051.
11. Bakkouri WE, Kania RE, Guichard JP, Lot G, Herman P, Huy PT. Conservative management of 386 cases of unilateral vestibular schwannoma: tumor growth and consequences for treatment. *J Neurosurg* 2009;110:662–9. doi: 10.3171/2007.5.16836.
12. Smouha EE, Yoo M, Mohr K, Davis RP. Conservative management of acoustic neuroma: a meta-analysis and proposed treatment algorithm. *Laryngoscope* 2005;115:450–4. doi: 10.1097/00005537-200503000-00011.
13. Perez-Rodriguez J, Lai S, Ehst BD, Fine DM, Bluemke DA. Nephrogenic systemic fibrosis: incidence, associations, and effect of risk factor assessment-report of 33 cases. *Radiology* 2009;250:371–7. doi: 10.1148/radiol.2502080498.
14. McDonald RJ, McDonald JS, Kallmes DF, Jentoft ME, Murray DL, Thielen KR, et al. Intracranial gadolinium deposition after contrast-enhanced MR imaging. *Radiology* 2015;275:772–82. doi: 10.1148/radiol.15150025.
15. Ramalho J, Semelka RC, Ramalho M, Nunes RH, AlObaidy M, Castillo M. Gadolinium-based contrast agent accumulation and toxicity: an update. *AJNR Am J Neuroradiol* 2016;37:1192–8. doi:10.3174/ajnr.A4615.
16. Forgues M, Mehta R, Anderson D, Morel C, Miller L, Sevy A, et al. Non-contrast magnetic resonance imaging for monitoring patients with acoustic neuroma. *J Laryngol Otol* 2018;132:780-5. doi: 10.1017/S0022215118001342.

17. Bayraktaroğlu S, Pabuçcu E, Ceylan N, Duman S, Savaş R, Alper H. Evaluation of the necessity of contrast in the follow-up MRI of schwannomas. *Diagn Interv Radiol* 2011;17:209–15. doi: 10.4261/1305-3825.DIR.3786-10.1.
18. Abele TA, Besachio DA, Quigley EP, Gurgel RK, Shelton C, Harnsberger HR, et al. Diagnostic accuracy of screening MR imaging using unenhanced axial CISS and coronal T2WI for detection of small internal auditory canal lesions. *AJNR Am J Neuroradiol* 2014 ;35:2366-70. doi: 10.3174/ajnr.A4041.
19. Ozgen B, Oguz B, Dolgun A. Diagnostic accuracy of the constructive interference in steady state sequence alone for follow-up imaging of vestibular schwannomas. *AJNR Am J Neuroradiol* 2009;30:985–91. doi: 10.3174/ajnr.A1472.
20. Walsh RM, Bath AP, Bance ML, Keller A, Rutka JA. Comparison of two radiologic methods for measuring the size and growth rate of extracanalicular vestibular schwannomas. *Am J Otol* 2000;21:716–21.
21. Zou J, Hirvonen T. “Wait and scan” management of patients with vestibular schwannoma and the relevance of non-contrast MRI in the follow-up. *J Otol* 2017;12:174–84. doi: 10.1016/j.joto.2017.08.002.
22. Pizzini FB, Sarno A, Galazzo IB, Fiorino F, Aragno AMR, Ciceri E, et al. Usefulness of high resolution T2-weighted images in the evaluation and surveillance of vestibular schwannoma? Is gadolinium needed?. *Otol Neurotol* 2020;41:e103-10. doi: 10.1097/MAO.0000000000002436.
23. Lawson McLean AC, McLean AL, Rosahl SK. Evaluating vestibular schwannoma size and volume on magnetic resonance imaging: an inter- and intra- rater agreement study. *Clin Neurol Neurosurg* 2016;145:68-73. doi: 10.1016/j.clineuro.2016.04.010.